Genetic and environmental influences on the size of specific brain regions in midlife: The VETSA MRI study

William S. Kremen [a,b,c,*], Elizabeth Prom-Wormley [d], Matthew S. Panizzon [a], Lisa T. Eyler [a,c], Bruce Fischl [e], Michael C. Neale [d], Carol E. Franz [a], Michael J. Lyons [f], Jennifer Pacheco [e], Michele E. Perry [a,g], Allison Stevens [e], J. Eric Schmitt [d], Michael D. Grant [f], Larry J. Seidman [h], Heidi W. Thermenos [h], Ming T. Tsuang [a,b,c], Seth A. Eisen [i], Anders M. Dale [j,k], Christine Fennema-Notestine [a,j]

[a] Department of Psychiatry, University of California, San Diego, 9500 Gilman Drive (MC 0738), La Jolla, CA 92093, USA
[b] Center for Behavioral Genomics, University of California, San Diego, La Jolla, CA
[c] VA San Diego Healthcare System, La Jolla, CA, USA
[d] Departments of Psychiatry and Human Genetics, Virginia Commonwealth University, Richmond, VA, USA
[e] Department of Radiology, Harvard Medical School and Massachusetts General Hospital, Boston, MA, USA
[f] Department of Psychology, Boston University, Boston, MA, USA
[g] Department of Cognitive Neuroscience, University of California, San Diego, La Jolla, CA, USA
[h] Department of Psychiatry, Harvard Medical School, Boston, MA, USA
[i] Department of Veterans Affairs, Washington, DC and Departments of Medicine and Psychiatry, Washington University, St. Louis, MO, USA
[j] Department of Radiology, University of California, San Diego, La Jolla, CA, USA
[k] Department of Neurosciences, University of California, San Diego, La Jolla, CA, USA

ARTICLE INFO

ABSTRACT

The impact of genetic and environmental factors on human brain structure is of great importance for understanding normative cognitive and brain aging as well as neuropsychiatric disorders. However, most studies of genetic and environmental influences on human brain structure have either focused on global measures or have had samples that were too small for reliable estimates. Using the classical twin design, we assessed genetic, shared environmental, and individual-specific environmental influences on individual differences in the size of 96 brain regions of interest (ROIs). Participants were 474 middle-aged male twins (202 pairs; 70 unpaired) in the Vietnam Era Twin Study of Aging (VETSA). They were 51–59 years old, and and were similar to U.S. men in their age range in terms of sociodemographic and health characteristics. We measured thickness of cortical ROIs and volume of other ROIs. On average, genetic influences accounted for approximately 70% of the variance in the volume of global, subcortical, and ventricular ROIs and approximately 45% of the variance in the thickness of cortical ROIs. There was greater variability in the heritability of cortical ROIs (0.00–0.75) as compared with subcortical and ventricular ROIs (0.48–0.85). The results did not indicate lateralized heritability differences or greater genetic influences on the size of regions underlying higher cognitive functions. The findings do provide key information for imaging genetic studies and other studies of brain phenotypes and endophenotypes. Longitudinal analysis will be needed to determine whether the degree of genetic and environmental influences changes for different ROIs from midlife to later life.

© 2009 Published by Elsevier Inc.

Elucidating the extent to which genetic and environmental factors influence adult brain structure is of great importance for understanding age-related normal and pathological changes in brain and cognition. Twin studies provide the optimal behavioral genetic method for clarifying this issue because they make it possible to decompose the variance of any variable into genetic, shared environmental influences, and individual-specific environmental influences. The twin method also complements molecular genetic approaches in that heritability – the proportion of phenotypic variance due to genes – is a key component for selection of phenotypes.

Despite many published magnetic resonance imaging (MRI) studies involving twins (reviewed by Glahn et al., 2007; Peper et al., 2007; Schmitt et al., 2007a), the picture regarding the heritability of specific brain regions remains incomplete. In some studies, samples sizes were quite small and are thus likely to provide unstable estimates (Visscher, 2004). With a couple of exceptions, relatively few specific regions of interest (ROIs) have been examined. The different ROIs that have been measured in previous studies have often been examined in different samples. It would be advantageous to be able to compare heritabilities of different ROIs in the same individuals, thus

* Corresponding author. Department of Psychiatry, University of California, San Diego, 9500 Gilman Drive (MC 0738), La Jolla, CA 92093, USA. Fax: +858 822 5856.
E-mail address: wkremen@ucsd.edu (W.S. Kremen).

circumventing the problem of variation of estimates due to differ- ences in sample characteristics or imaging methods. Assessing all of the ROIs within the same individual allows for direct comparison of one brain structure to another.

Examination of a large number of ROIs in the same people has been performed in a small study of adults in which 92 ROIs (46 per hemisphere) plus total brain volume and lateral ventricles were examined in 9 monozygotic (MZ) and 10 dizygotic (DZ) twin pairs (Wright et al., 2002), and the large NIMH twin sample of children and adolescents (126 twin pairs plus siblings) in which ROIs throughout the neocortex plus a few subcortical and ventricular ROIs were measured (Wallace et al., 2006 #1845; Lenroot et al., 2007 #1999; Schmitt, 2008 #1998). Another large study of children (105 nine- year-old twin pairs) examined global brain measures plus the lateral ventricles and cerebellum (Peper et al., 2009).

We are aware of only two relatively large published adult MRI twin samples: a sample of older men (NHLBI study; 145 pairs) (Carmelli et al., 1998) and a Dutch adult sample (112 pairs) (Posthuma et al., 2000). These samples focused mainly on global brain measures or a few selected ROIs. To our knowledge, the present study is the first large-scale study to include a comprehensive assessment of genetic and environmental influences on cortical, subcortical, and ventricular ROIs all in the same individuals. We refer here specifically to ROI-based analyses. We are aware of important studies using point-by-point gray matter density analyses or voxel- based methods (e.g., Hulshoff Pol et al., 2006; Peper et al., 2009; Thompson et al., 2001), but we have not focused on these here, in part, because they are not very comparable to ROI-based analyses (see Discussion).

In adults, heritabilities tend to be very high for global measures, averaging around 80% or more for whole-brain volume, total gray matter, and total white matter (Carmelli et al., 1998; Posthuma et al., 2000; Wright et al., 2002). The heritability of lateral ventricular volume has yielded very mixed findings with estimates ranging from 0% to 78% (Baaré et al., 2001; Carmelli et al., 2002; Chou et al., 2008; Schmitt et al., 2007b; Wright et al., 2002). The heritability of hippocampal volume has been estimated at 40% in older adults and 66%–71% in younger and middle-aged adults (Sullivan et al., 2001; van Erp et al., 2004; Wright et al., 2002). The heritability of cerebellar volume was 66%–67% in younger adults and 81% in middle-aged adults (Posthuma et al., 2000; Wright et al., 2002).

In the case of children and adolescents, Pennington et al. (2000) reported monozygotic (MZ) and dizygotic (DZ) twin correlations that suggest heritabilities of approximately 80% for total brain volume and 66% and 56% for right and left hemisphere volumes, respectively. In the NIMH sample, heritabilities ranged from 77% to 89% for total gray and white matter and lobar volumes (Wallace et al., 2006). Heritabilities were 80% for the caudate nucleus (Wallace et al., 2006), 72% for thalamus, 81% for basal ganglia, 55% for total cerebellum volume, and 32% for lateral ventricles (Schmitt et al., 2007b). All but the caudate were subsequently analyzed controlling for total brain volume or intracranial volume; these analyses resulted in lower heritabilities of 42% for thalamus, 64% for basal ganglia, 24% for cerebellum, and 17% for the lateral ventricles (Lenroot et al., 2007; Schmitt et al., 2007b, 2008). The average heritability of the thickness of 54 cortical ROIs (27 per hemisphere) in the NIMH sample was 32% (range: 1%–57%). Estimates of shared environmental variance were zero or near zero for virtually all of the cortical and subcortical ROIs.

In the present study, the Vietnam Era Twin Study of Aging (VETSA), we comprehensively assessed the heritability of 96 brain ROIs in 404 middle-aged male twins (202 pairs). Specification of this as a midlife sample with a narrow age range is important because gene expression may be age dependent, and different genetically mediated processes may affect brain structure at different ages because of substantial brain growth and development during childhood and processes influencing loss of brain tissue in adults. Because the same phenotype may be influenced by different genetic factors at different developmental stages, such potential age-related differences may also have important implications for genetic association studies. However, the present analyses do not address age-related changes because these data represent only the first wave of this longitudinal study of genetic and environmental contributions to cognitive and brain aging.

Methods

Participants

An overview of the longitudinal VETSA project can be found elsewhere (Kremen et al., 2006). The study was approved by the Human Subjects Committees of all involved institutions, and all participants gave written informed consent. A total of 1237 twins participated in wave 1. They were randomly selected from a larger pool of individuals in a prior Vietnam Era Twin Registry study (Tsuang et al., 2001). Registry members are male–male twin pairs born between 1939 and 1957 who both served in the United States military between 1965 and 1975. The registry is not a VA or a patient sample, and the large majority was not in Vietnam or exposed to combat. Registry members are currently middle-aged men living throughout the United States. We began the VETSA MRI study in the third year of the primary VETSA study. At the time of this report, there were 474 individual VETSA participants with analyzable MRI data; 241 were scanned in San Diego and 231 were scanned in Boston. Of those, 404 were paired (i.e., 202 twin pairs): 110 MZ and 92 DZ pairs. The unpaired twins contribute to the calculations of means and variances, but the focus of the genetic analyses is the paired twins. Zygosity was initially classified according to questionnaire and blood group information. These classifications are being updated on the basis of 25 satellite markers. To date, 56% of the MRI study participants have DNA-determined zygosity. Consistent with the overall VETSA project, 95% of the questionnaire/blood group-based classifications were in agreement with the DNA-based classifications; when differences occurred we used the DNA-based classifications.

Participants were given the option of traveling to San Diego or Boston for a day-long series of assessments. The MRI session was typically the day after the in-lab evaluation. Only 6% of VETSA participants who were invited to undergo MRI declined to participate; 59% were included. The remaining participants were excluded from the MRI study for reasons such as possible metal in the body (7%), claustrophobia (3%), unwillingness to travel to the MRI study sites (5%), scanner problems (8%), co-twin being excluded (9%), and other reasons (3%).

Mean age of the MRI participants was 55.8 (2.6) years (range: 51– 59), mean years of education was 13.9 (SD = 2.1), and 85.2% were right-handed. Most participants were employed full-time (74.9%), 4.2% were employed part-time, and 11.2% were retired. There were 88.3% non-Hispanic white, 5.3% African-American, 3.4% Hispanic, and 3.0% "other" participants. Self-reported overall health status was as follows: excellent (14.8%); very good (36.5%); good (37.4%); fair (10.4%); and poor (0.9%). These demographic characteristics did not differ from the entire VETSA sample, nor were there significant differences between MZ and DZ twins. Basic demographic and health characteristics of the VETSA sample are comparable to U.S. census data for similarly aged men. For example, the prevalence of hypertension and diabetes in American men between 2003 and 2006 based on reports of diagnosis by a doctor was 41.2% and 9.6%, respectively (National Centers for Disease Control and Prevention, 2003–2006); the corresponding prevalences for the VETSA sample were 39% and 11%.

Image acquisition

Images were acquired on Siemens 1.5 Tesla scanners (241 at University of California, San Diego; 233 at Massachusetts General Hospital). Sagittal T1-weighted MPRAGE sequences were employed with a TI = 1000 ms, TE = 3.31 ms, TR = 2730 ms, flip angle = 7 degrees, slice thickness = 1.33 mm, and voxel size = $1.3 \times 1.0 \times 1.3$ mm. Raw DICOM MRI scans (including two T1-weighted volumes per case) were downloaded to the MGH site. Images were automatically corrected for spatial distortion caused by gradient nonlinearity and B_1 field inhomogeneity. The two T1-weighted images were registered and averaged to improve signal-to-noise.

Image processing

Volumetric segmentation (Fischl et al., 2002, 2004a) and cortical surface reconstruction (Dale et al., 1999; Dale and Sereno, 1993; Fischl et al., 1999, 2002, 2004a,b) methods were based on the publicly available FreeSurfer software package. The semi-automated, fully 3D whole-brain segmentation procedure uses a probabilistic atlas and applies a Bayesian classification rule to assign a neuroanatomical label to each voxel (Fischl et al., 2002, 2004a). A widely used training atlas has been shown to be comparable to that of expert manual labeling and is sensitive to subtle brain changes in Alzheimer's disease and normal aging (Fischl et al., 2002, 2004a). However, we created a new manually derived training set from 20 unrelated, randomly selected VETSA participants. Both atlases were created at the same laboratory at the MGH Center for Morphometric analysis using the same reliability criteria. The rationale for the VETSA-specific atlas was that it would be more representative of the VETSA sample, thus yielding more accurate measurements. As an example, Fig. 1 shows the results of different versions of the general atlas and the VETSA-specific atlas for some subcortical and global structures in comparison to the "gold standard," manually segmented brains. The figure shows the ROIs based on each atlas in standard deviation units from the manually segmented brains. The zero-point represents the manual measurements. As can be seen, the VETSA-specific atlas yielded the most accurate measurements, all of which were very close to the manual measurements and within the 99% confidence intervals (CIs). In addition, FreeSurfer provides an estimate of total intracranial volume (TIV) derived from the atlas scaling factor on the basis of the transformation of the full brain mask into atlas space (Buckner et al.,
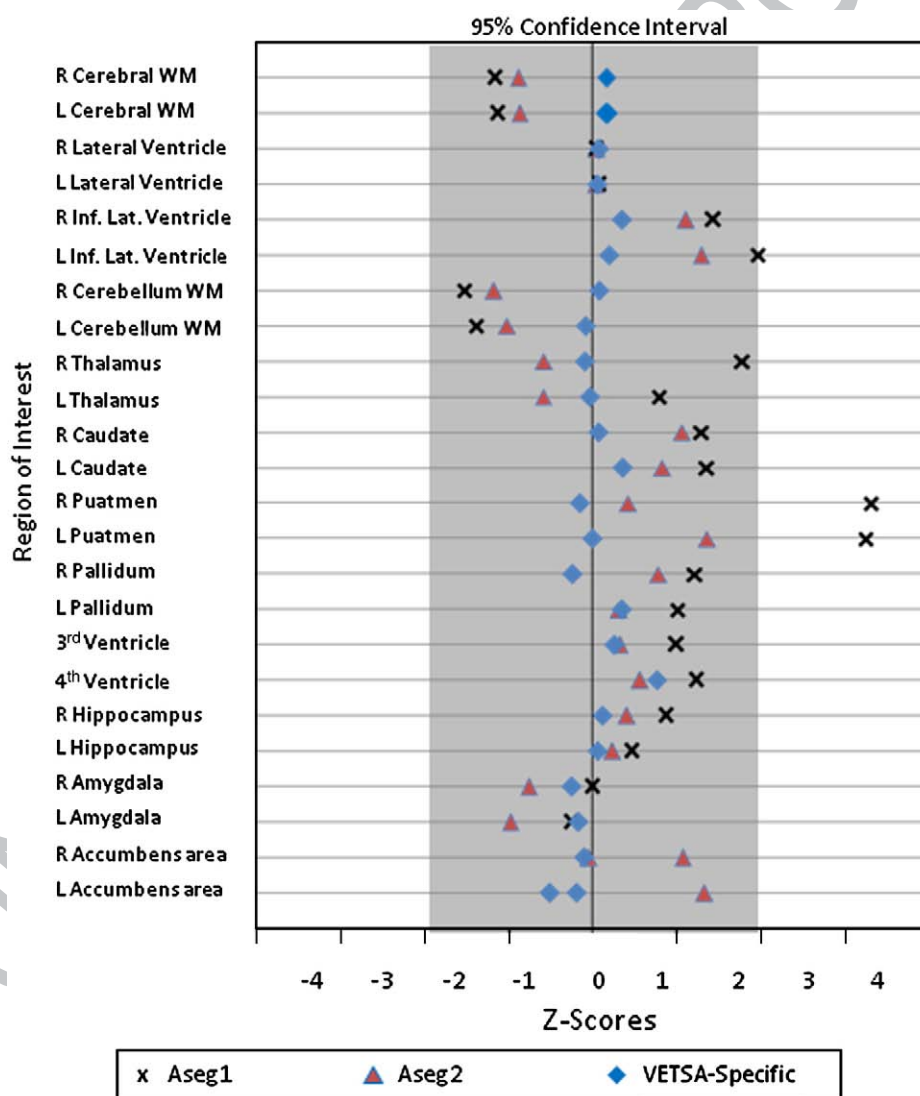

Fig. 1. FreeSurfer automated segmentation compared with expert manual measurements based on VETSA-specific and other atlases. ASeg 1 refers to the initial automated segmentation results based on the atlas of Buckner et al. (2004). ASeg 2 refers to automated segmentation after updates in the FreeSurfer processing stream. VETSA refers to automated segmentation based on the VETSA-specific atlas. The center vertical line at $Z = 0$ represents the manual segmentation measurements, which were done at the MGH Center for Morphometric Analysis for both atlases.

2004). TIV was used to control for differences in head size for volumetric measures.

Volume measures

Volumetric measures were created for hippocampus, amygdala, caudate, putamen, thalamus, nucleus accumbens, cerebellum, ventricles, cerebral cortex, cerebral white matter, and abnormal hypointense white matter regions. Measured white matter abnormalities reflect areas within the white matter that have abnormally low, or hypointense, signal values relative to normal white matter; these areas are analogous to the more commonly referenced hyperintensities derived from T2-weighted images and may reflect areas of inflammation, demyelination, or axonal loss.

Cortical thickness measures

Using semi-automated cortical surface reconstruction methods (Dale et al., 1999; Dale and Sereno, 1993; Fischl and Dale, 2000; Fischl et al., 1999, 2004b) available in FreeSurfer, we measured thickness at each surface location, or vertex. Intensity variations due to magnetic field inhomogeneities are corrected, a normalized intensity image is created, and the skull (non-brain) is removed from the normalized image. The preliminary segmentation is partitioned using a connected components algorithm, with connectivity not allowed across the established cutting planes that separate the cerebral hemispheres and disconnect brainstem and cerebellum. Any interior holes in the components representing white matter are filled, resulting in a single filled volume for each cortical hemisphere. The resulting surface is covered with a triangular tessellation and smoothed to reduce metric distortions. After the initial surface model has been constructed, a refinement procedure is applied to obtain a representation of the gray/white boundary. This surface is subsequently deformed outwards to obtain an explicit representation of the pial surface.

The surface was then divided into distinct cortical ROIs (Fischl et al., 2004b). Each surface location, or vertex, was assigned a neuroanatomical label based on (1) the probability of each label at each location in a surface-based atlas space, based on a manually parcellated training set; (2) the local curvature information; and (3) the contextual information, encoding spatial neighborhood relationships between labels (conditional probability distributions derived from the manual training set). The parcellation scheme labels cortical sulci and gyri according to Desikan et al. (2006), and thickness values are calculated in the 66 ROIs (33 per hemisphere) produced by this parcellation. We renamed the regions referred to as the posterior and isthmus cingulate in the original parcellation scheme (Desikan et al., 2006); these are referred to here as the rostral posterior cingulate and retrosplenial cortex, respectively. We also use the term "subcortical" as a shorthand for the following cerebral gray matter ROIs that are not included in the cortical surface reconstruction: thalamus, caudate, putamen, pallidum, nucleus accumbens, hippocampus, and amygdala.

Quality control

Dr. Dale and colleagues developed and refined the image acquisition and processing methods for the present study in conjunction with the Morphometry Biomedical Informatics Research Network (BIRN; http://www.nbirn.net/research/morphometry/index.shtm), which is sponsored by the National Institutes of Health and the National Center for Research Resources. A major goal of the BIRN is to develop tools to enable cross-site and cross-platform reliability, and BIRN-affiliated studies have consistently demonstrated the reliability and validity of these image acquisition and processing methods across different sites and platforms (Dickerson et al., 2008; Fennema-Notestine et al., 2007; Han et al., 2006; Jovich et al., 2006, 2009). Once generated, the cortical surface model is visually inspected and edited for technical accuracy by trained technicians. Minimal manual editing – blind to any participant characteristics – was performed in alignment with standard, objective editing rules. Studies demonstrate a high correlation of automatic and manual measures in vivo and ex vivo (Fischl and Dale, 2000; Walhovd et al., 2005). Qualitative review of the volumetric segmentation was also performed to check for technical failure of the application. Of the 493 scans available at the time of these analyses, quality control measures excluded 0.6% (3 cases) due to scanner artifact and 3% (16 cases) due to inadequate image processing results (e.g., poor contrast caused removal of non-brain to fail).

Statistical analysis

ROI volume or thickness was adjusted for age and site in all analyses. Although site effects on the means of MRI measures were observed for some regions, these made very little difference to the estimates of heritability (results available on request). In addition, volume measures were analyzed with and without adjustment for TIV. The primary focus was on analyses adjusted for TIV because we wanted to examine heritabilities for specific ROIs over and above general effects of head size and because most studies report values based on similar adjustments. The primary emphasis for analyses of cortical thickness did not include any adjustment for TIV because, as shown in the Results section, adjusting cortical thickness for ICV had virtually no effect on heritability. All of the ventricular and white matter hypointensity measures were log transformed in order to normalize their distributions.

The standard twin ("ACE") model estimates the proportion of phenotypic variance due to additive genetic effects (A), shared or common environmental effects (C), and individual-specific environmental effects (E) (Eaves et al., 1978; Neale and Cardon, 1992). Shared environmental influences are those that make twins similar; individual-specific environmental influences are those that make twins different. Because measurement error is assumed to be random, it is uncorrelated within twin pairs; consequently; it is included in the individual-specific environmental variance. Fig. 2 shows the basic univariate ACE model: (1) additive genetic factors correlate 1.0 for MZ twins and 0.5 for DZ twins; (2) shared environmental factors correlate 1.0 across twins regardless of zygosity; and (3) individual-specific environmental factors are uncorrelated across twins. The fit of the models to the data was tested by means of Mx, a maximum-likelihood-based structural equation modeling program (Neale et al., 2003).

If MZ correlations are substantially more than double the DZ correlations, non-additive (dominant/epistatic) genetic influences may also be operating. These effects can be incorporated into an "ADE" model in which D refers to non-additive/dominance genetic
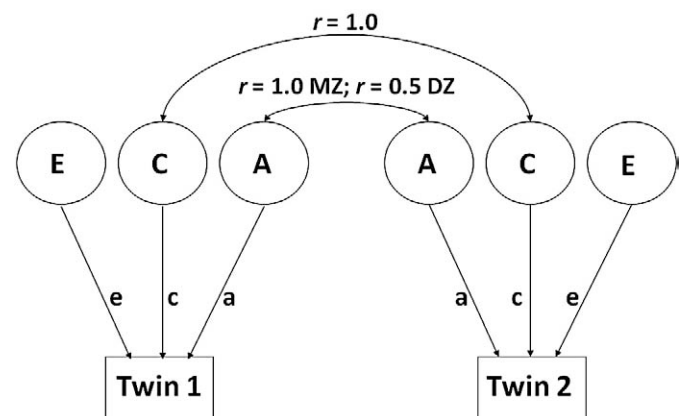

Fig. 2. Univariate ACE model. A = Additive genetic influences; C = Shared (common) environmental influences; E = Individual-specific (unique) environmental influences. a, c, and e = parameter estimates for A, C, and E, respectively.

effects; in the ADE model, non-additive genetic factors are assumed to correlate 0.25 in DZ twins. We first compared the fit of the full (ACE or ADE) models with saturated models, which are models that fit the data perfectly. For only 3 of the 97 (ROIs including TIV) was the fit of the full model significantly worse than the fit of the saturated model; there were for right cerebral cortex, white matter hypointensities, and left pericalcarine cortex). Because this outcome is fewer than would be expected by chance, based on an alpha level of 0.05, we consider the model testing to be appropriate. These results are not presented here but are available from the authors. We did not have sufficient power to differentiate between A and D effects in the ADE models, but broad heritability estimates (A+D) were extremely similar to estimates based on the A component in the corresponding ACE models. We present only the ACE models so that it is easier to compare results across ROIs. ADE model results are available from the authors.

After fitting univariate ACE models for each ROI, we tested the significance of each A, C, and E parameter by dropping each from the model. This procedure produces nested submodels in which the difference in maximum likelihood asymptotically follows a χ^2 distribution with degrees of freedom equal to the difference in the number of free parameters in most cases (Eaves et al., 1978; Neale and Cardon, 1992). Models were compared using the likelihood-ratio chi-square (LRC) statistic. The LRC is obtained by comparing the -2 log-likelihood (-2LL) of the comparison model to the -2LL of a nested (reduced) model. The LRC statistic is the difference in -2LL. A significant LRC indicates that the component removed from the model accounts for a statistically significant proportion of variance.

Results

MZ and DZ correlations and the proportions of variance accounted for by genetic, shared environmental, and individual-specific environmental influences for each of the age, site, and TIV-adjusted volume-based ROIs are shown in Table 1. The same indices for the ROIs measured by thickness (adjusted for age and site only) are shown in Table 2 and in Fig. 3. MZ correlations were consistently higher than DZ correlations, suggesting genetic influences on the size of almost all ROIs. The full (ACE) models are shown, although the estimates of shared environmental (C) effects were near zero in most cases. On average in the full models, individual-specific environmental influences accounted for 29% of the variance in the size of specific subcortical ROIs and 51% of the variance in the size of specific cortical ROIs.

Table 1
Regional brain volume measures adjusted for age, site, and total intracranial volume: parameter estimates for univariate ACE Models and tests of submodels.

Region of interest	rMZ	rDZ	Variance components								p-values		
			a^2	95% CI	c^2	95% CI	e^2	95% CI	-2Lnl		no A	no C	no AC
Global measures													
Total intracranial volume[a]	0.80	0.49	0.79	(0.52; 0.87)	0.04	(0; 0.30)	0.17	(0.13; 0.23)	1020.68		**<0.0001**	0.79	<0.0001
Cerebral cortex—L	0.83	0.39	0.77	(0.40; 0.85)	0.10	(0; 0.40)	0.20	(0.14; 0.27)	749.50		**<0.0001**	1.00	<0.0001
Cerebral cortex—R	0.76	0.33	0.70	(0.51; 0.83)	0.00	(0; 0.22)	0.24	(0.17; 0.34)	716.04		**<0.0001**	0.58	<0.0001
Cerebral WM—L	0.76	0.36	0.76	(0.46; 0.83)	0.00	(0; 0.27)	0.25	(0.18; 0.35)	688.84		**<0.0001**	1.00	<0.0001
Cerebral WM—R	0.63	0.04	0.75	(0.45; 0.73)	0.00	(0; 0.08)	0.38	(0.27; 0.55)	676.67		**<0.0001**	1.00	<0.0001
WM hypointensities	0.83	0.39	0.62	(0.44; 0.83)	0.00	(0; 0.32)	0.23	(0.17; 0.31)	1017.61		**<0.0001**	1.00	<0.0001
Subcortical gray matter regions[b]													
Thalamus—L	0.68	0.35	0.68	(0.35; 0.77)	0.00	(0; 0.29)	0.32	(0.23; 0.43)	893.37		**<0.0001**	1.00	<0.0001
Thalamus—R	0.71	0.48	0.60	(0.30; 0.81)	0.14	(0; 0.41)	0.26	(0.19; 0.35)	869.31		**<0.0001**	0.36	<0.0001
Caudate—L	0.87	0.52	0.79	(0.54; 0.91)	0.09	(0; 0.34)	0.12	(0.09; 0.17)	807.28		**<0.0001**	0.53	<0.0001
Caudate—R	0.82	0.47	0.70	(0.43; 0.86)	0.11	(0; 0.37)	0.19	(0.14; 0.26)	856.31		**<0.0001**	0.49	<0.0001
Putamen—L	0.86	0.42	0.85	(0.56; 0.90)	0.01	(0; 0.29)	0.14	(0.10; 0.19)	881.26		**<0.0001**	0.96	<0.0001
Putamen—R	0.85	0.34	0.84	(0.63; 0.88)	0.00	(0; 0.21)	0.16	(0.12; 0.22)	890.61		**<0.0001**	1.00	<0.0001
Pallidum—L	0.69	0.41	0.66	(0.33; 0.78)	0.05	(0; 0.34)	0.29	(0.22; 0.40)	927.95		**<0.0001**	0.78	<0.0001
Pallidum—R	0.76	0.33	0.75	(0.44; 0.81)	0.00	(0; 0)	0.25	(0.19; 0.34)	941.07		**<0.0001**	1.00	<0.0001
Nucleus accumbens—L	0.64	0.12	0.60	(0.39; 0.70)	0.00	(0; 0)	0.40	(0.30; 0.53)	1045.27		**<0.0001**	1.00	<0.0001
Nucleus accumbens—R	0.53	0.15	0.48	(0.14; 0.60)	0.00	(0; 0)	0.52	(0.40; 0.66)	1080.91		**0.01**	1.00	<0.0001
Hippocampus—L	0.66	0.21	0.63	(0.36; 0.72)	0.00	(0; 0)	0.37	(0.28; 0.49)	975.32		**0.00**	1.00	<0.0001
Hippocampus—R	0.70	0.05	0.64	(0.47; 0.74)	0.00	(0; 0.14)	0.36	(0.27; 0.47)	955.97		**<0.0001**	1.00	<0.0001
Amygdala—L	0.65	0.27	0.63	(0.28; 0.72)	0.00	(0; 0.31)	0.37	(0.28; 0.49)	990.35		**0.00**	1.00	<0.0001
Amygdala—R	0.69	0.25	0.66	(0.33; 0.74)	0.00	(0; 0.30)	0.34	(0.26; 0.45)	969.31		**0.0002**	1.00	<0.0001
Cerebellum													
Cerebellum cortex—L	0.77	0.41	0.64	(0.33; 0.81)	0.11	(0; 0.40)	0.25	(0.18; 0.33)	916.02		**<0.0001**	0.53	<0.0001
Cerebellum cortex—R	0.81	0.38	0.76	(0.44; 0.85)	0.03	(0; 0.34)	0.21	(0.15; 0.28)	914.60		**<0.0001**	0.87	<0.0001
Cerebellum WM—L	0.82	0.29	0.79	(0.54; 0.84)	0.00	(0; 0.23)	0.21	(0.16; 0.29)	877.48		**<0.0001**	1.00	<0.0001
Cerebellum WM—R	0.83	0.28	0.81	(0.61; 0.86)	0.00	(0; 0.19)	0.19	(0.14; 0.26)	882.03		**<0.0001**	1.00	<0.0001
Ventricles													
Lateral ventricle—L	0.79	0.11	0.76	(0.63; 0.82)	0.00	(0; 0.11)	0.24	(0.18; 0.33)	928.65		**<0.0001**	1.00	<0.0001
Lateral ventricle—R	0.76	0.22	0.73	(0.53; 0.80)	0.00	(0; 0.18)	0.27	(0.20; 0.37)	948.68		**<0.0001**	1.00	<0.0001
Inf. lateral ventricle—L	0.68	0.19	0.65	(0.40; 0.73)	0.00	(0; 0.21)	0.35	(0.27; 0.47)	1029.27		**<0.0001**	1.00	<0.0001
Inf. lateral ventricle—R	0.39	0.10	0.37	(0.02; 0.51)	0.00	(0; 0.27)	0.63	(0.49; 0.79)	1077.54		**0.04**	1.00	<0.0001
3rd ventricle	0.76	0.42	0.79	(0.52; 0.85)	0.00	(0; 0)	0.21	(0.15; 0.28)	946.32		**<0.0001**	1.00	<0.0001
4th ventricle	0.76	0.28	0.75	(0.53; 0.81)	0.00	(0; 0.19)	0.25	(0.19; 0.35)	1025.94		**<0.0001**	1.00	<0.0001

a^2 = additive genetic influences; c^2 = shared (common) environmental influences; e^2 = individual-specific (unique) environmental influences; CI = confidence interval; -2Lnl = -2 log-likelihood for the full model; no A = test of CE model, i.e., hypothesis of no additive genetic (A) effects; no C = test of AE model, i.e., hypothesis of no shared environmental effects; no AC = test of E only model, i.e., hypothesis of no familial (additive genetic or shared environmental) effects; WM = white matter; Inf. = inferior.
Significant genetic influences based on ACE models ($p<0.05$ in "no A" column) are shown in bold font.
[a] Total intracranial volume is adjusted for age and site only.
[b] Use of the term subcortical is a shorthand for these cerebral gray matter ROIs that are not included in the cortical surface reconstruction.

Table 2
Regional cortical thickness measures adjusted for age and site: parameter estimates for univariate ACE models and tests of submodels.

Region of interest	rMZ	rDZ	a^2	95% CI	c^2	95% CI	e^2	95% CI	−2Lnl	no A	no C	no AC
Frontal lobe												
Superior frontal gyrus—L	0.79	0.21	0.75	(0.53; 0.81)	0.00	(0; 0.21)	0.25	(0.19; 0.34)	1003.70	**<0.0001**	1.00	<0.0001
Superior frontal gyrus—R	0.72	0.26	0.68	(0.33; 0.76)	0.00	(0; 0.32)	0.32	(0.24; 0.42)	1026.60	**0.0001**	1.00	<0.0001
Middle frontal gyrus												
Rostral division—L	0.48	0.13	0.45	(0.15; 0.58)	0.00	(0; 0.24)	0.55	(0.42; 0.70)	1076.41	**0.01**	1.00	<0.0001
Rostral division—R	0.53	0.23	0.52	(0.16; 0.63)	0.00	(0; 0.30)	0.48	(0.37; 0.62)	1072.43	**0.01**	1.00	<0.0001
Caudal division—L	0.63	0.06	0.57	(0.35; 0.67)	0.00	(0; 0.17)	0.43	(0.33; 0.56)	1089.44	**0.0001**	1.00	<0.0001
Caudal division—R	0.60	0.36	0.41	(0.03; 0.68)	0.17	(0; 0.50)	0.42	(0.32; 0.55)	1083.08	**0.04**	0.37	<0.0001
Inferior frontal gyrus												
Pars opercularis—L	0.64	0.23	0.62	(0.36; 0.72)	0.00	(0; 0.23)	0.38	(0.28; 0.50)	1075.05	**0.0001**	1.00	<0.0001
Pars opercularis—R	0.42	0.08	0.37	(0; 0.50)	0.00	(0; 0.31)	0.63	(0.50; 0.78)	1099.11	**0.05**	1.00	<0.0001
Pars triangularis—L	0.48	0.13	0.44	(0.08; 0.57)	0.00	(0; 0.31)	0.56	(0.43; 0.70)	1126.59	**0.02**	1.00	<0.0001
Pars triangularis—R	0.44	0.06	0.40	(0.14; 0.54)	0.00	(0; 0.20)	0.60	(0.46; 0.75)	1119.28	**0.01**	1.00	<0.0001
Pars orbitalis—L	0.42	0.07	0.37	(0.08; 0.51)	0.00	(0; 0.22)	0.63	(0.49; 0.79)	1086.29	**0.02**	1.00	<0.0001
Pars orbitalis—R	0.48	0.20	0.47	(0.13; 0.59)	0.00	(0; 0.27)	0.53	(0.41; 0.68)	1115.41	**0.01**	1.00	<0.0001
Orbitofrontal cortex												
Lateral division—L	0.50	0.12	0.47	(0.21; 0.59)	0.00	(0; 0.20)	0.53	(0.41; 0.68)	1067.63	**0.003**	1.00	<0.0001
Lateral division—R	0.56	0.07	0.52	(0.32; 0.64)	0.00	(0; 0.15)	0.48	(0.36; 0.63)	1097.87	**0.0002**	1.00	<0.0001
Medial division—L	0.38	0.11	0.35	(0; 0.49)	0.00	(0; 0.32)	0.65	(0.51; 0.80)	1126.70	0.07	1.00	<0.0001
Medial division—R	0.39	0.17	0.39	(0; 0.53)	0.00	(0; 0.30)	0.61	(0.47; 0.77)	1111.77	**0.05**	1.00	<0.0001
Frontal pole—L	0.37	0.01	0.32	(0.07; 0.47)	0.00	(0; 0.17)	0.68	(0.53; 0.86)	1131.85	**0.02**	1.00	0.00
Frontal pole—R	0.17	0.01	0.14	(0; 0.31)	0.00	(0; 0.20)	0.86	(0.69; 1.00)	1128.59	0.33	1.00	0.30
Precentral gyrus—L	0.37	−0.01	0.66	(0.43; 0.74)	0.00	(0; 0.19)	0.34	(0.26; 0.45)	1064.42	**<0.0001**	1.00	<0.0001
Precentral gyrus—R	0.17	0.01	0.60	(0.22; 0.73)	0.05	(0; 0.38)	0.35	(0.27; 0.46)	1045.79	**0.00**	0.78	<0.0001
Paracentral lobule—L	0.69	0.20	0.62	(0.26; 0.71)	0.00	(0; 0.32)	0.38	(0.29; 0.49)	1074.72	**0.001**	1.00	<0.0001
Paracentral lobule—R	0.67	0.34	0.64	(0.37; 0.73)	0.00	(0; 0.25)	0.36	(0.27; 0.47)	1071.23	**<0.0001**	1.00	<0.0001
Parietal lobe												
Postcentral gyrus—Postcentral Gyrus – L	0.63	0.21	0.59	(0.26; 0.69)	0.00	(0; 0.29)	0.41	(0.31; 0.53)	1074.82	**0.001**	1.00	<0.0001
Postcentral gyrus—R	0.71	0.20	0.65	(0.33; 0.73)	0.00	(0; 0.29)	0.35	(0.27; 0.46)	1053.04	**0.0002**	1.00	<0.0001
Supramarginal Gyrus—L	0.61	0.23	0.58	(0.21; 0.68)	0.00	(0; 0.32)	0.42	(0.32; 0.54)	1083.97	**0.003**	1.00	<0.0001
Supramarginal Gyrus—R	0.56	0.15	0.51	(0.19; 0.63)	0.00	(0; 0.28)	0.49	(0.37; 0.62)	1094.60	**0.004**	1.00	<0.0001
Superior parietal cortex—L	0.64	0.24	0.62	(0.30; 0.71)	0.00	(0; 0.28)	0.38	(0.29; 0.50)	1060.71	**0.0005**	1.00	<0.0001
Superior parietal cortex—R	0.70	0.15	0.67	(0.47; 0.75)	0.00	(0; 0.17)	0.33	(0.25; 0.44)	1049.06	**<0.0001**	1.00	<0.0001
Inferior parietal cortex—L	0.67	0.23	0.65	(0.37; 0.74)	0.00	(0; 0.24)	0.35	(0.26; 0.46)	1026.90	**<0.0001**	1.00	<0.0001
Inferior parietal cortex—R	0.52	0.16	0.50	(0.18; 0.61)	0.00	(0; 0.26)	0.50	(0.39; 0.65)	1064.35	**0.01**	1.00	<0.0001
Precuneus—L	0.71	0.09	0.66	(0.47; 0.74)	0.00	(0; 0.15)	0.34	(0.26; 0.46)	1085.46	**<0.0001**	1.00	<0.0001
Precuneus—R	0.64	0.07	0.57	(0.33; 0.67)	0.00	(0; 0.21)	0.43	(0.33; 0.55)	1073.97	**0.0003**	1.00	<0.0001
Occipital lobe												
Lingual gyrus—L	0.57	0.28	0.57	(0.19; 0.67)	0.00	(0; 0.32)	0.43	(0.33; 0.56)	1072.86	**0.004**	1.00	<0.0001
Lingual gyrus—R	0.61	0.27	0.60	(0.28; 0.70)	0.00	(0; 0.27)	0.40	(0.30; 0.53)	1059.52	**0.001**	1.00	<0.0001
Pericalcarine cortex—L	0.57	−0.09	0.46	(0.27; 0.58)	0.00	(0; 0.15)	0.54	(0.42; 0.68)	1107.95	**0.001**	1.00	<0.0001
Pericalcarine cortex—R	0.43	0.15	0.39	(0; 0.51)	0.00	(0; 0.39)	0.61	(0.49; 0.76)	1100.20	0.11	1.00	<0.0001
Cuneus—L	0.59	0.02	0.51	(0.27; 0.62)	0.00	(0; 0.20)	0.49	(0.38; 0.62)	1076.76	**0.001**	1.00	<0.0001
Cuneus—R	0.62	0.17	0.57	(0.26; 0.67)	0.00	(0; 0.27)	0.43	(0.33; 0.56)	1062.02	**0.001**	1.00	<0.0001
Lateral occipital cortex—L	0.61	0.17	0.57	(0.27; 0.67)	0.00	(0; 0.25)	0.43	(0.33; 0.56)	1073.60	**0.001**	1.00	<0.0001
Lateral occipital cortex—R	0.59	0.16	0.55	(0.26; 0.65)	0.00	(0; 0.25)	0.45	(0.35; 0.58)	1064.85	**0.001**	1.00	<0.0001
Temporal lobe												
Lateral aspect												
Superior temporal gyrus—L	0.60	0.03	0.53	(0.33; 0.64)	0.00	(0; 0.16)	0.47	(0.36; 0.60)	1098.14	**0.0002**	1.00	<0.0001
Superior temporal gyrus—R	0.71	0.34	0.54	(0.18; 0.74)	0.12	(0; 0.45)	0.33	(0.25; 0.44)	1036.85	**0.003**	0.54	<0.0001
Middle temporal gyrus—L	0.44	0.10	0.39	(0.02; 0.52)	0.00	(0; 0.31)	0.61	(0.48; 0.76)	1093.45	**0.04**	1.00	<0.0001
Middle temporal gyrus—R	0.45	0.21	0.46	(0.05; 0.58)	0.00	(0; 0.32)	0.54	(0.42; 0.70)	1082.33	**0.03**	1.00	<0.0001
Inferior temporal gyrus—L	0.45	0.25	0.45	(0.01; 0.58)	0.00	(0; 0.35)	0.55	(0.42; 0.71)	1075.43	**0.04**	1.00	<0.0001
Inferior temporal gyrus—R	0.51	0.35	0.40	(0; 0.66)	0.14	(0; 0.46)	0.45	(0.34; 0.60)	1059.33	**0.05**	0.43	<0.0001
Transv. temporal cortex—L	0.58	0.21	0.58	(0.32; 0.68)	0.00	(0; 0.20)	0.42	(0.32; 0.56)	1100.85	**0.0004**	1.00	<0.0001
Transv. temporal cortex—R	0.55	0.12	0.50	(0.19; 0.61)	0.00	(0; 0.26)	0.50	(0.39; 0.64)	1101.37	**0.005**	1.00	<0.0001
Banks Sup. Temp. sulcus—L	0.02	0.09	0.00	(0; 0.22)	0.05	(0; 0.19)	0.95	(0.78; 1.00)	1129.39	1.00	0.61	0.74
Banks Sup. Temp. sulcus—R	0.21	0.15	0.08	(0; 0.37)	0.13	(0; 0.32)	0.79	(0.63; 0.95)	1099.91	0.76	0.57	0.02
Medial aspect												
Entorhinal cortex—L	0.32	0.28	0.21	(0; 0.51)	0.14	(0; 0.40)	0.65	(0.49; 0.82)	1127.90	0.40	0.46	<0.0001
Entorhinal cortex—R	0.38	0.19	0.34	(0; 0.52)	0.04	(0; 0.39)	0.62	(0.48; 0.79)	1095.55	0.17	0.84	<0.0001
Parahippocampal gyrus—L	0.44	0.24	0.46	(0; 0.59)	0.01	(0; 0.37)	0.53	(0.41; 0.70)	1084.41	**0.05**	1.00	<0.0001
Parahippocampal gyrus—R	0.56	0.22	0.55	(0.24; 0.66)	0.00	(0; 0.25)	0.45	(0.34; 0.58)	1075.46	**0.002**	1.00	<0.0001
Temporal pole—L	0.56	−0.03	0.47	(0.26; 0.59)	0.00	(0; 0.17)	0.53	(0.41; 0.67)	1082.58	**0.001**	1.00	<0.0001
Temporal pole—R	0.32	−0.07	0.25	(0; 0.40)	0.00	(0; 0.20)	0.75	(0.60; 0.92)	1112.59	0.06	1.00	0.01
Fusiform gyrus—L	0.47	0.20	0.46	(0.05; 0.58)	0.00	(0; 0.33)	0.54	(0.42; 0.69)	1048.02	**0.03**	1.00	<0.0001
Fusiform gyrus—R	0.52	0.28	0.54	(0.12; 0.65)	0.00	(0; 0.34)	0.46	(0.35; 0.61)	1045.61	**0.01**	1.00	<0.0001

Table 2 (continued)

Region of interest	rMZ	rDZ	Variance components								p-values		
t2.80			a^2	95% CI	c^2	95% CI	e^2	95% CI	−2Lnl	no A	no C	no AC
Cingulate cortex												
Rostral anterior division—L	0.25	0.16	0.14	(0; 0.40)	0.10	(0; 0.33)	0.76	(0.60; 0.92)	1117.04	0.61	0.65	0.01
Rostral anterior division—R	0.22	0.27	0.00	(0; 0.36)	0.24	(0; 0.37)	0.76	(0.62; 0.89)	1118.24	1.00	0.14	<0.0001
Caudal anterior division—L	0.23	0.28	0.00	(0; 0.38)	0.26	(0; 0.38)	0.74	(0.60; 0.88)	1129.26	1.00	0.14	<0.0001
Caudal anterior division—R	0.45	0.13	**0.43**	(0.12; 0.56)	0.00	(0; 0.24)	0.57	(0.44; 0.72)	1103.94	0.01	1.00	<0.0001
Rostral posterior division—L	0.43	0.15	**0.42**	(0.04; 0.55)	0.00	(0; 0.31)	0.58	(0.45; 0.73)	1102.90	0.03	1.00	<0.0001
Rostral posterior division—R	0.48	0.07	**0.47**	(0.21; 0.60)	0.00	(0; 0.20)	0.53	(0.40; 0.68)	1074.89	0.003	1.00	<0.0001
Retrosplenial cortex—L	0.56	0.21	**0.54**	(0.20; 0.65)	0.00	(0; 0.28)	0.46	(0.35; 0.59)	1100.87	0.003	1.00	<0.0001
Retrosplenial cortex—R	0.47	0.35	0.20	(0; 0.58)	0.27	(0; 0.52)	0.53	(0.41; 0.68)	1106.43	0.34	0.18	<0.0001

a^2 = additive genetic influences; c^2 = shared (common) environmental influences; e^2 = individual-specific (unique) environmental influences; CI = Confidence interval; −2Lnl = −2 log-likelihood for full the model; no A = test of CE model, i.e., hypothesis of no additive genetic (A) effects; no C = test of AE model, i.e., hypothesis of no shared environmental effects; no AC = test of E only model, i.e., hypothesis of no familial (additive genetic or shared environmental) effects; Transv. = transverse; Sup. Temp. = superior temporal.
Significant genetic influences based on ACE models (p< 0.05 in "no A" column) are shown in **bold** font.

Unadjusted volume measures

Global volumes measures, subcortical gray matter ROIs (thalamus, caudate, putamen, pallidum, hippocampus, amygdala, nucleus accumbens), and ventricular measures were generally highly heritable. The average heritabilities for these three groups of measures were 0.82, 0.73, and 0.71, respectively.

Volume measures adjusted for TIV

The average heritability of the global volume measures was 0.72. Heritabilities for total gray matter and white matter volumes ranged from 0.70 to 0.77, and the heritability of white matter hypointensity volume was 0.62. The mean heritability of subcortical gray matter ROIs was 0.68 for both left–right hemisphere regions (range = 0.48–0.85). These tended to be highest in basal ganglia structures (putamen, caudate, pallidum), with a range of 0.66 to 0.85. The next highest heritabilities were in limbic and diencephalic regions (hippocampus, amygdala, thalamus), with a range of 0.60 to 0.68. The average heritability of ventricular measures was 0.68. The reductions in heritability for these volume measures after adjusting for TIV averaged 8%.

Cortical thickness measures

The average heritability of the individual ROIs within each major lobe was 0.60 for parietal, 0.53 for occipital, 0.49 for frontal, and 0.40 for temporal. The average left–right difference was less than
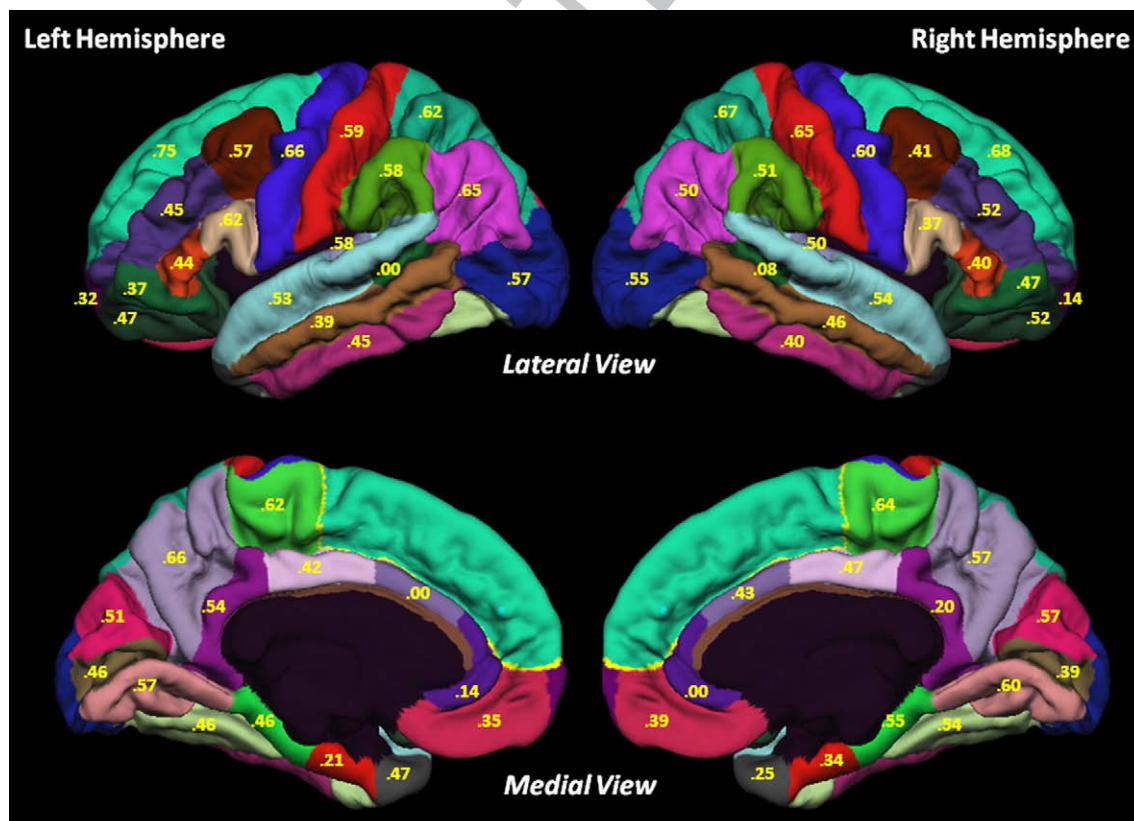

Fig. 3. Heritabilities of the thickness of specific cortical ROIs defined according to Desikan et al. (2006).

0.01 for each of the major lobes. The average heritabilities were not different for the lateral (0.39) and medial (0.41) aspects of the temporal lobe. Average heritability of thickness for all specific cortical ROIs was 0.47 in the left hemisphere and 0.45 in the right hemisphere (range = 0.00–0.75). Heritability was moderate for parahippocampal gyrus (0.46 left; 0.55 right) but lower for entorhinal cortex (0.21 left; 0.34 right). The average heritability of the cingulate cortex thickness was 0.29 for both the left and the right hemisphere, but there was considerable variability with estimates ranging from 0.00 to 0.54.

Cortical volume measures

Our focus was on thickness, but many studies report volume measures of cortical ROIs. The overall average heritability of the unadjusted cortical ROI volumes was 0.44 compared with 0.46 for the overall average for thickness ROIs. Adjusting for TIV did not affect cortical thickness heritability (mean = 0.45), but it did reduce average cortical volume heritability to 0.31. This constitutes an average reduction of 30% for the heritability of cortical volumes compared with only 2% for cortical thickness.

False discovery rate

Significance of the heritabilities can be determined by the column showing no A effects or by the 95% CIs in the tables. All of the heritabilities for global, subcortical, and other volume-based ROIs were statistically significant. In total, there were 96 ROIs, and based on the ACE models, 91 of the 96 ROIs (95%) had significant heritability at the $p < 0.05$ level. As defined by Benjamini and Hochberg (1995), the false discovery rate is determined by computing a_i by ranking the p-value of each of the n tests from smallest (p_1) to largest (p_n) and multiplying each p-value by n divided by the rank (i) of that p-value ($a_i = p_i*n/i$). If we allow for a 5% false discovery rate, all tests for which $a_i < 0.05$ would be considered as significant. Based on that criterion, only 4 out of 91 ROIs would be considered false discoveries. Even those four would be considered marginally significant, with a_i values ranging from 0.053 to 0.055. Because the C estimates were near zero in most cases, it was possible to drop C without any significant loss in model fit. In the resulting AE models, the 95% CIs for the A components were much narrower than they were in ACE models and only two had p-values >0.05. The AE models may also be useful for comparison with other reports; see Supplementary Table 1 for volume-based measures and Supplementary Table 2 for cortical thickness measures. Finally, homologous regions in the left and right hemispheres tended to have very similar heritabilities. There was considerable overlap in the 95% CIs for all homologous left–right pairings, suggesting that differences in heritability were not significant.

Discussion

To our knowledge, this is the first large-scale study to comprehensively examine genetic and environmental influences on the size of specific cortical, subcortical, and ventricular brain structures all in the same individuals. On average, about 70% of the variance in the size of subcortical ROIs and ventricles is determined by genetic factors. Cortical ROIs showed a moderate degree of genetic influence, accounting, on average, for about 45% of the variance in thickness. There was also greater variability among the cortical ROIs, with heritabilities ranging from 0.00 to 0.75 compared with 0.48 to 0.85 for the subcortical ROIs. On average, heritabilities for homologous left hemisphere and right hemisphere regions were roughly equivalent.

Cortical thickness measures

The left and right hemisphere similarities are consistent with the NIMH child and adolescent sample. The average heritability of all specific cortical ROIs of 0.46 in the present study was somewhat higher than the average of 0.31 in the NIMH sample. With regard to specific cortical regions, superior frontal gyrus, pre- and postcentral gyri, and supramarginal gyrus were among those with the highest heritabilities in both studies. However, there were also several inconsistencies regarding specific regions with the highest or lowest heritabilities. The results in the present study were not especially consistent with those of Wright et al. (2002), but their sample size of only 19 twin pairs may be unlikely to provide reliable heritability estimates.

There are also voxel-based or point-by-point analyses of brain structure. We have performed similar analyses in other work with the VETSA sample (unpublished data), but such analyses to be readily comparable to ROI-based analyses. For example, Thompson et al. (2001) examined a continuous map of gray matter density (i.e., proportion of voxels classified as gray matter), so that there are not ROIs that can be compared with the present study. Many of the heritabilities reported in that study were between 0.90 and 1.00, higher than any observed in the present study. Heritabilities in homologous left and right regions were reported to be significantly higher in Wernicke's areas than in its right hemisphere homologue. However, as stated by Thompson et al. (2001), "With a sample size of only 40 twins, heritability coefficients cannot be estimated precisely, and limited statistical power precludes the detection of differences in heritability between individual regions of cortex." Hulshoff Pol et al. (2006) identified 14 gray matter density voxels with significant heritability and the regions in which they were located, but it may be misleading to compare significant heritability in a few voxels within an ROI versus the heritability of the entire ROI. Indeed, if the other voxels within the ROI were not significantly heritable, the logical conclusion may be that the size of that ROI as a whole is not heritable. Also, in these studies, dramatic adjustments were made to the family-wise error rate to correct for multiple testing. That approach protects against any type I error but substantially increases the risk of failing to detect true effects. In our study, we controlled the expected false discovery rate, i.e., the proportion of significant results that are actually type I errors. That analysis indicated that 79 of 83 significant heritabilities were likely to be truly significant. Given the prior literature on the heritability of brain structures, it is reasonable to expect that most ROIs would be heritable.

In contrast to our detailed characterization of cortical thickness, we presented only a brief summary of results for cortical volume measures. An advantage of cortical thickness is that, unlike cortical volume measures, heritability estimates were unrelated to TIV. Consequently, the difficulties of interpreting adjusted versus unadjusted ROIs are avoided for cortical thickness measures. Elsewhere, we have shown that cortical thickness and surface area are determined by largely independent sets of genes; because volume is basically the product of thickness and surface area, it is not possible to separate these two sources of genetic variance if the phenotype is cortical volume (Panizzon et al., 2009). Analysis of genetic and environmental influences on the surface area of each of the cortical ROIs is the subject of a separate article.

Volume measures

The present results are consistent with two of three reports for hippocampal volume (Sullivan et al., 2001; van Erp et al., 2004; Wright et al., 2002). Our heritability estimates for cerebellar volume were fairly similar to that of another large adult twin sample (Posthuma et al., 2000), but they were substantially lower in the NIMH sample (Wallace et al., 2006). The most extreme variability across studies is in the heritability of the lateral ventricles. Our

estimate of 0.78 (left–right average) was similar to that of an older adult sample (Carmelli et al., 2002), but varied substantially from that of two younger adult samples that yielded estimates of zero (Baaré et al., 2001; Wright et al., 2002), and the estimate of 0.17 from the NIMH sample (Schmitt et al., 2007b; Wallace et al., 2006).

Accounting for differences in heritability

Previous results on a more limited set of ROIs suggest that sex differences are unlikely to account for the observed differences between the VETSA and other samples (Baaré et al., 2001). Nevertheless, this provides only a limited test of sex effects. Differences in image acquisition, image processing, and definition of ROIs could account for differences across studies. Also, except for the NIMH study, other studies measured cortical volume or gray matter density rather than cortical thickness. Age differences are another possible reason for differences across studies. Heritabilities were somewhat higher in the present study compared with the NIMH sample, and there could be a tendency for the heritability to increase from adolescence to adulthood as has been suggested for some other phenotypes (McClearn et al., 1997). It is also noteworthy that subcortical heritabilities measured in the NIMH child and adolescent sample were reduced by 21% and 42% after adjusting for total brain volume, but only by an average of 7% after adjusting for TIV in the present adult sample. This difference may reflect the impact of developmental factors in the child and adolescent sample as there is still growth of total brain volume and TIV during this period (Courchesne et al., 2000).

Comparison of the middle-aged VETSA sample and the NHLBI sample indicates very similar heritabilities of 0.78 for left and 0.70 for right lateral ventricle size in that older sample (Carmelli et al., 2002). Heritability of white matter abnormalities in the NHLBI sample was 0.71 (Carmelli et al., 1998) compared with 0.62 in VETSA. Average heritability of hippocampal volume was 0.64 in VETSA and 0.40 in the NHLBI study (Sullivan et al., 2001). Differences could be due to methodological factors such as the use of T1-weighted images in VETSA and T2-weighted images in the NHLBI study to measure white matter abnormalities. In any case, the direction of age-related differences in heritability is not consistent for these different ROIs. A more definitive answer to the question of how genetic and environmental influences on brain structure change beyond midlife must await longitudinal assessments as are planned in the VETSA projects.

Although the heritability estimates for lateral ventricle volumes were highest in the two older samples, it is not clear that there is a simple increase in heritability with age because the lateral ventricles showed the greatest inconsistency across studies. The inconsistency is intriguing, in part, because the lateral ventricles are one of the easiest ROIs to measure reliably. The degree of genetic versus environmental control of lateral ventricular size may be particularly important for aging-related disorders of cognition such as Alzheimer's disease or for psychotic disorders such as schizophrenia, both of which are associated with parenchymal shrinkage and ventricular enlargement. Key questions to be addressed will be whether these two processes are determined by the same or different sets of genetic influences, and whether change in one or both is more environmentally determined.

It has been suggested that brain regions that are most important for higher cognitive functions have higher heritabilities (Lenroot et al., 2007; Thompson et al., 2001). Given that the brain is designed for adaptation and learning, the opposite viewpoint seems equally plausible. There is empirical evidence indicating that environmental manipulations can influence human brain structure (Draganski et al., 2004). It may be adaptive for brain regions that are most important for higher cognitive functions to be most malleable in response to environmental influences. Development of language-related abilities, for example, is contingent upon considerable environmental input. In the present study, the thickness of language-related cortical regions was generally not more highly heritable than other regions. Conversely, the thickness of some prefrontal regions, which underlie some of the highest cognitive functions, were among the most highly heritable. Thus, it does not appear that the extent of genetic influences on the size of neuroanatomic regions maps onto the complexity of cognitive function in any straightforward way. From an evolutionary perspective, one might expect that genetic variance (and thus, heritability) would be low for older structures because natural selection processes might be nearer to "completion" for those structures (Falconer, 1989). However, subcortical ROIs had higher heritabilities relative to cortical ROIs in both children (NIMH sample) and middle-aged adults (present sample).

Environmental factors

Despite our emphasis on genetic factors, environmental factors do play a major role as well, accounting for over one-half of the variance in the thickness of cortical regions, and over one-quarter of the variance in subcortical regions. In almost all cases, the environmental influences were individual specific, not shared. In general, power to detect shared environmental effects in twin studies is relatively low, but the fact that the estimates of shared environmental effects were often near zero suggests that the lack of significant effects was not due to insufficient power.

Limitations

The present study has some limitations that should be noted. We cannot be certain about generalizability of the findings to women. As stated in the methods section, our index of TIV is an estimated measure, although Buckner et al. (2004) have shown that the one-parameter scaling factor implemented in FreeSurfer does provide a reasonable TIV estimation that is correlated with manual TIV measurements. This issue is relevant to only a subset of volumetric ROIs that included adjustment for TIV, and most of the heritability estimates for those measures did tend to be comparable to those found in other studies. FreeSurfer's index of white matter hypointensities based on T1-weighted images almost certainly underestimates white matter abnormalities compared with measures derived from T2-weighted indices of hyperintensities. It is not clear in what direction, if any, this might affect heritability estimates. Although not an optimal measure, we do have evidence for the construct validity of our white matter hypointensity measure in that it is correlated with hypertension and some cognitive measures in ways that are similar to findings based on standard T2-weighted hyperintensity measures (unpublished data).

One might consider it a limitation that VETSA participants were not screened for exclusion criteria other than MRI safety considerations. These and other illness/injury factors are typically exclusion criteria for neuroimaging studies because they are viewed as confounds. On the other hand, that means that what is mostly known about brain aging is about highly screened segment of the population—what has sometimes been referred to as "super-normal" (Kendler, 1990). The epidemiological approach taken in the present study was to minimize screening, and as noted in the methods section the VETSA sample is similar to American men in terms of overall health characteristics. Illnesses or injuries are not regarded as confounds. Rather, they are additional factors contributing to the total genetic and environmental variances that influence the size of brain structures. This approach does not mean that the role of specific factors in contributing to the heritability of brain structure is unimportant, but the examination of those relationships requires multiple separate analyses that are beyond the scope of this article.

Elsewhere we have noted advantages of examining patterns in continuous maps of cortical thickness that are not constrained by

traditional ROI boundaries (Rimol et al., 2007), although it is important to examine genetic and environmental influences on the basis of traditional ROIs as well. These types of ROIs are widely used, and they do have anatomical and functional significance and provide comparison for much existing work. Moreover, subcortical structures without the layered structure of the cortex are less amenable to continuous maps.

Implications

The considerable variability in heritability across individual ROIs provides insight toward a better understanding of the effect of genes on brain structure and function, an important goal in the post-genomic era. The findings are also relevant to candidate gene and genetic association studies because they contribute important information regarding brain endophenotypes that might be used in the study of cognitive and brain aging as well as neurological and psychiatric disorders. Future work may elucidate the genetic architecture across different brain regions in multivariate analyses, and longitudinal analyses may reveal changes in genetic and environmental influences that take place in normal and pathological brain aging.

Acknowledgments

Appendix A. Supplementary data

Supplementary data associated with this article can be found, in the online version, at doi:10.1016/j.neuroimage.2009.09.043.

References

Baaré, W.F.C., Hulshoff Pol, H.F., Boomsma, D.I., Posthuma, D., de Geus, E.J.C., Schnack, H. G., van Haren, N.E.M., van Oel, C.J., Kahn, R.S., 2001. Quantitative genetic modeling of variation in human brain morphology. Cereb. Cortex 11, 816–824.

Benjamini, Y., Hochberg, Y., 1995. Controlling the false discovery rate: a practical and powerful approach to multiple testing. J. R. Stat. Soc. Ser. B (Methodological) 57, 289–300.

Buckner, R.L., Head, D., Parker, J., Fotenos, A.F., Marcus, D., Morris, J.C., Snyder, A.Z., 2004. A unified approach for morphometric and functional data analysis in young, old, and demented adults using automated atlas-based head size normalization: reliability and validation against manual measurement of total intracranial volume. NeuroImage 23, 724–738.

Carmelli, D., DeCarli, C., Swan, G.E., Jack, L.M., Reed, T., Wolf, P.A., Miller, B.L., 1998. Evidence for genetic variance in white matter hyperintensity volume in normal elderly male twins. Stroke 29, 1177–1181.

Carmelli, D., Swan, G.E., DeCarli, C., Reed, T., 2002. Quantitative genetic modeling of regional brain volumes and cognitive performance in older male twins. Biol. Psychol. 61, 139–155.

Chou, Y.Y., Lepore, N., Chiang, M.C., Avedissian, C., Barysheva, M., McMahon, K.L., de Zubicaray, G.I., Meredith, M., Wright, M.J., Toga, A.W., Thompson, P.M., 2008. Mapping genetic influences on ventricular structure in twins. NeuroImage 44, 1312–1323.

Courchesne, E., Chisum, H.J., Townsend, J., Cowles, A., Covington, J., Egaas, B., Harwood, M., Hinds, S., Press, G.A., 2000. Normal brain development and aging: quantitative analysis at in vivo MR imaging in healthy volunteers. Radiology 216, 672–682.

Dale, A.M., Sereno, M.I., 1993. Improved localization of cortical activity by combining EEG and MEG with MRI cortical surface reconstruction: a linear approach. J. Cogn. Neurosci. 5, 162–176.

Dale, A.M., Fischl, B., Sereno, M.I., 1999. Cortical surface-based analysis. I: segmentation and surface reconstruction. NeuroImage 9, 179–194.

Desikan, R.S., Segonne, F., Fischl, B., Quinn, B.T., Dickerson, B.C., Blacker, D., Buckner, R.L., Dale, A.M., Maguire, R.P., Hyman, B.T., Albert, M.S., Killiany, R.J., 2006. An automated labeling system for subdividing the human cerebral cortex on MRI scans into gyral based regions of interest. NeuroImage 31, 968–980.

Dickerson, B.C., Fenstermacher, E., Salat, D.H., Wolk, D.A., Maguire, R.P., Desikan, R., Pacheco, J., Quinn, B.T., Van der Kouwe, A., Greve, D.N., Blacker, D., Albert, M.S., Killiany, R.J., Fischl, B., 2008. Detection of cortical thickness correlates of cognitive performance: reliability across MRI scan sessions, scanners, and field strengths. NeuroImage 39, 10–18.

Draganski, B., Gaser, C., Busch, V., Schuierer, G., Bogdahn, U., May, A., 2004. Neuroplasticity: changes in grey matter induced by training. Nature 427, 311–312.

Eaves, L.J., Last, K.A., Young, P.A., Martin, N.G., 1978. Model-fitting approaches to the analysis of human behavior. Heredity 41, 249–320.

Falconer, D.S., 1989. Introduction to Quantitative Genetics, 3rd ed. Longsman Green/ Wiley, Essex, UK.

Fennema-Notestine, C., Gamst, A.C., Quinn, B.T., Pacheco, J., Jernigan, T.L., Thal, L., Buckner, R., Killiany, R., Blacker, D., Dale, A.M., Fischl, B., Dickerson, B., Gollub, R.L., 2007. Feasibility of multi-site clinical structural neuroimaging studies of aging using legacy data. Neuroinformatics 5, 235–245.

Fischl, B., Dale, A.M., 2000. Measuring the thickness of the human cerebral cortex from magnetic resonance images. Proc. Natl. Acad. Sci. 97, 11050–11055.

Fischl, B., Sereno, M.I., Dale, A.M., 1999. Cortical surface-based analysis. II: inflation, flattening, and a surface-based coordinate system. NeuroImage 9, 195–207.

Fischl, B., Salat, D.H., Busa, E., Albert, M., Dieterich, M., Haselgrove, C., van der Kouwe, A., Killiany, R., Kennedy, D., Klaveness, S., Montillo, A., Makris, N., Rosen, B., Dale, A.M., 2002. Whole brain segmentation: automated labeling of neuroanatomical structures in the human brain. Neuron 33, 341–355.

Fischl, B., Salat, D.H., van der Kouwe, A.J., Makris, N., Segonne, F., Quinn, B.T., Dale, A.M., 2004a. Sequence-independent segmentation of magnetic resonance images. NeuroImage 23 (Suppl. 1), S69–S84.

Fischl, B., van der Kouwe, A., Destrieux, C., Halgren, E., Segonne, F., Salat, D.H., Busa, E., Seidman, L.J., Goldstein, J., Kennedy, D., Caviness, V., Makris, N., Rosen, B., Dale, A.M., 2004b. Automatically parcellating the human cerebral cortex. Cereb. Cortex 14, 11–22.

Glahn, D.C., Thompson, P.M., Blangero, J., 2007. Neuroimaging endophenotypes: strategies for finding genes influencing brain structure and function. Hum. Brain Mapp. 28, 488–501.

Han, X., Jovicich, J., Salat, D., van der Kouwe, A., Quinn, B., Czanner, S., Busa, E., Pacheco, J., Albert, M., Killiany, R., Maguire, P., Rosas, D., Makris, N., Dale, A., Dickerson, B., Fischl, B., 2006. Reliability of MRI-derived measurements of human cerebral cortical thickness: the effects of field strength, scanner upgrade and manufacturer. NeuroImage 32, 180–194.

Hulshoff Pol, H.E., Schnack, H.G., Posthuma, D., Mandl, R.C., Baare, W.F., van Oel, C., van Haren, N.E., Collins, D.L., Evans, A.C., Amunts, K., Burgel, U., Zilles, K., de Geus, E., Boomsma, D.I., Kahn, R.S., 2006. Genetic contributions to human brain morphology and intelligence. J. Neurosci. 26, 10235–10242.

Jovicich, J., Czanner, S., Greve, D., Haley, E., van der Kouwe, A., Gollub, R., Kennedy, D., Schmitt, F., Brown, G., Macfall, J., Fischl, B., Dale, A.M., 2006. Reliability in multi-site structural MRI studies: effects of gradient non-linearity correction on phantom and human data. NeuroImage 30, 436–443.

Jovicich, J., Czanner, S., Han, X., Salat, D., van der Kouwe, A., Quinn, B., Pacheco, J., Albert, M., Killiany, R., Blacker, D., Maguire, P., Rosas, D., Makris, N., Gollub, R., Dale, A., Dickerson, B.C., Fischl, B., 2009. MRI-derived measurements of human subcortical, ventricular and intracranial brain volumes: reliability effects of scan sessions, acquisition sequences, data analyses, scanner upgrade, scanner vendors and field strengths. NeuroImage. [Q1]

Kendler, K.S., 1990. The super-normal control group in psychaitric genetics: possible artifactual evidence for coaggregation. Psychiatr. Genet. 1, 45–53.

Kremen, W.S., Thompson-Brenner, H., Leung, Y.J., Grant, M.D., Franz, C.E., Eisen, S.A., Jacobson, K.C., Boake, C., Lyons, M.J., 2006. Genes, environment, and time: The Vietnam Era Twin Study of Aging (VETSA). Twin Res. Hum. Genet. 9, 1009–1022.

Lenroot, R.K., Schmitt, J.E., Ordaz, S.J., Wallace, G.L., Neale, M.C., Lerch, J.P., Kendler, K.S., Evans, A.C., Giedd, J.N., 2007. Differences in genetic and environmental influences on the human cerebral cortex associated with development during childhood and adolescence. Hum. Brain Mapp. [Q2]

McClearn, G.E., Johansson, B., Berg, S., Pedersen, N.L., Ahern, F., Petrill, S.A., Plomin, R., 1997. Substantial genetic influence on cognitive abilities in twins 80 or more years old. Science 276, 1560–1563.

National Centers for Disease Control and Prevention, 2003–2006. Health Data Interactive. National Center for Health Statistics, Hyattsville, MD.

Neale, M.C., Cardon, L.R., 1992. Methodology for Genetic Studies of Twins and Families. Kluwer Academic Publishers, Dordrecht, The Netherlands.

Neale, M.C., Boker, S.M., Xie, G., Maes, H.H., 2003. Mx: Statistical Modeling, 6th ed. Department of Psychiatry, Medical College of Virginia, Richmond, VA.

Panizzon, M.S., Fennema-Notestine, C., Eyler, L.T., Jernigan, T.L., Prom-Wormley, E., Neale, M., Jacobson, K., Lyons, M.J., Grant, M.D., Franz, C.E., Xian, H., Tsuang, M., Fischl, B., Seidman, L., Dale, A., Kremen, W.S., 2009. Distinct genetic influences on cortical surface area and cortical thickness. Cereb. Cortex.

Pennington, B.F., Filipek, P.A., Lefly, D., Chhabildas, N., Kennedy, D.N., Filley, C.M., Galabura, A., DeFries, J.C., 2000. A twin MRI study of size variations in the human brain. J. Cogn. Neurosci. 12, 223–232.

Peper, J.S., Brouwer, R.M., Boomsma, D.I., Kahn, R.S., Hulshoff Pol, H.E., 2007. Genetic influences on human brain structure: a review of brain imaging studies in twins. Hum. Brain Mapp. 28, 464–473.

Peper, J.S., Schnack, H.G., Brouwer, R.M., Van Baal, G.C., Pjetri, E., Szekely, E., van Leeuwen, M., van den Berg, S.M., Collins, D.L., Evans, A.C., Boomsma, D.I., Kahn, R.S., Hulshoff Pol, H.E., 2009. Heritability of regional and global brain structure at the onset of puberty: a magnetic resonance imaging study in 9-year-old twin pairs. Hum. Brain Mapp. 30, 2184–2196.

Posthuma, D., de Geus, E.J.C., Neale, M.C., Hulshoff Pol, H.E., Baare, W.E.C., Kahn, R.S., Boomsma, D., 2000. Multivariate genetic analysis of brain structure in an extended twin design. Behav. Genet. 30, 311–319.

Rimol, L.R., Kremen, W.S., Hagler, D.J.J., Fennema-Notestine, C., Eyler, L.T., Panizzon, M.S., Neale, M.C., Schmitt, J.E., Lyons, M.J., Franz, C.E., Fischl, B., Seidman, L.J., Makris, N., Perry, M.E., Pacheco, J., Dale, A.M., 2007. Heritability of cortical thickness in a large adult twin sample: The VETSA Project. Annual meeting of the Organization for Human Brain Mapping, Chicago, IL.

Schmitt, J.E., Eyler, L.T., Giedd, J.N., Kremen, W.S., Kendler, K.S., Neale, M.C., 2007a. Review of twin and family studies on neuroanatomic phenotypes and typical neurodevelopment. Twin Res. Hum. Genet. 10, 683–694.

Schmitt, J.E., Wallace, G.L., Rosenthal, M.A., Molloy, E.A., Ordaz, S., Lenroot, R., Clasen, L.S., Blumenthal, J.D., Kendler, K.S., Neale, M.C., Giedd, J.N., 2007b. A multivariate analysis of neuroanatomic relationships in a genetically informative pediatric sample. NeuroImage 35, 70–82.

Schmitt, J.E., Lenroot, R.K., Wallace, G.L., Ordaz, S., Taylor, K.N., Kabani, N., Greenstein, D., Lerch, J.P., Kendler, K.S., Neale, M.C., Giedd, J.N., 2008. Identification of genetically mediated cortical networks: a multivariate study of pediatric twins and siblings. Cereb. Cortex.

Sullivan, E.V., Pfefferbaum, A., Swan, G.E., Carmelli, D., 2001. Heritability in hippocampal size in elderly twin men: equivalent influence from genes and environment. Hippocampus 11, 754–762.

Thompson, P.M., Cannon, T.D., Narr, K.L., van Erp, T., Poutanen, V.P., Huttunen, M., Lonnqvist, J., Standertskjold-Nordenstam, C.G., Kaprio, J., Khaledy, M., Dail, R., Zoumalan, C.I., Toga, A.W., 2001. Genetic influences on brain structure. Nat. Neurosci. 4, 1253–1258.

Tsuang, M.T., Bar, J.L., Harley, R.M., Lyons, M.J., 2001. The Harvard Twin Study of Substance Abuse: what we have learned. Harv. Rev. Psychiatr. 9, 267–279.

van Erp, T.G., Saleh, P.A., Huttunen, M., Lonnqvist, J., Kaprio, J., Salonen, O., Valanne, L., Poutanen, V.P., Standertskjold-Nordenstam, C.G., Cannon, T.D., 2004. Hippocampal volumes in schizophrenic twins. Arch. Gen. Psychiatr. 61, 346–353.

Visscher, P.M., 2004. Power of the classical twin design revisited. Twin Res. 7, 505–512.

Walhovd, K.B., Fjell, A.M., Reinvang, I., Lundervold, A., Fischl, B., Salat, D., Quinn, B.T., Makris, N., Dale, A.M., 2005. Cortical volume and speed-of-processing are complementary in prediction of performance intelligence. Neuropsychologia 43, 704–713.

Wallace, G.L., Schmitt, J.E., Lenroot, R., Viding, E., Ordaz, S., Rosenthal, M.A., Molloy, E.A., Clasen, L.S., Kendler, K.S., Neale, M.C., Giedd, J.N., 2006. A pediatric twin study of brain morphometry. Eaves, L.J. 47, 987–993.

Wright, I.C., Sham, P., Murray, R.M., Weinberger, D.R., Bullmore, E.T., 2002. Genetic contributions to regional variability in human brain structure: methods and preliminary results. NeuroImage 17, 256–271.